

# Correlation for Predicting Corrosivity of Crude Oils Using Proton Nuclear Magnetic Resonance and Chemometric Methods

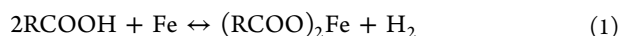
Carlos Mejia-Miranda,<sup>\*,†</sup> Dionisio Laverde,<sup>†</sup> and Daniel Molina V.<sup>‡</sup>

<sup>†</sup>Laboratorio de Corrosión, and <sup>‡</sup>Laboratorio de Resonancia Magnética Nuclear, Universidad Industrial de Santander, Apartado Aéreo 678, Bucaramanga, Santander, Colombia

**ABSTRACT:** Naphthenic acids and sulfur compounds cause corrosion problems in the crude distillation units. Their heterogeneity in the concentration and reactivity makes it difficult to predict the corrosivity of crude oils. In this paper, the areas of resonance signals belonging to 12 chemical shift regions of the proton nuclear magnetic resonance (<sup>1</sup>H NMR) spectra of crude oils were correlated with the corrosion rate of AISI SAE 1005 carbon steel using a partial least squares regression. The corrosion rates were determined by weight loss tests at 350 °C for 12 h. In addition, a correlation to calculate the corrosion rate based only on the acidity and sulfur percentage of crude oils was proposed for the same crude oil samples. A statistical comparison of the proposed correlations indicates that the <sup>1</sup>H NMR-based correlation has better quality in predicting corrosivity of crude oils. The combination of <sup>1</sup>H NMR spectroscopy with chemometric techniques provides a fast alternative method for quantitative prediction of the corrosion rate at typical operation temperatures of crude distillation units.

## 1. INTRODUCTION

Because of the significant decrease in the world reserves of conventional crude oils, the fraction of the so-called non-conventional or opportunity crude oils has increased in blends entering the crude distillation units (CDUs) in refineries.<sup>1</sup> High acidic crude oils, i.e., crude oils with high naphthenic acid (NA) content, and sour crude oils (high sulfur compound content) belong to non-conventional crude oils. Their processing leads to corrosion problems in the CDU, particularly in the lines between the heating furnaces and the distillation towers at temperatures between 220 and 400 °C.<sup>2–5</sup> The combined corrosive effects of NAs and sulfur-containing compounds are summarized in the following chemical reactions:<sup>3–6</sup>



The formation of soluble iron naphthenate by the interaction of NAs with the metallic materials is described by [reaction 1](#). [Reaction 2](#) describes the interaction of hydrogen sulfide with the metal, which forms solid iron sulfide that is deposited at the metallic surface. Hydrogen sulfide can also react with iron naphthenates to form iron sulfide and regenerate the NAs described by [reaction 3](#). Other reactions, such as thermal decomposition of NAs and sulfur compounds, might occur simultaneously at the same temperature conditions. The total acid number (TAN) and weight percent of sulfur (% SUL) are parameters used in the oil industry to represent the concentration of NAs and sulfur compounds, respectively. The TAN is defined as the milligrams of KOH required to neutralize 1 g of crude oil.<sup>2–6</sup> The values of TAN and % SUL in crude oils are used in the refinery to establish strategies for corrosion control. However, it has been proposed that the corrosivity of crude oils is not always associated with the TAN and the content of sulfur alone; also, the molecular structure of

these species is an important factor influencing the corrosivity of crude oils.<sup>4–8</sup> Because of the complexity of the reactions involved in the corrosion mechanism, it is difficult to develop reliable correlations to predict corrosion trends. Moreover, the composition of the mixtures entering the CDU constantly varies because it depends upon the changing supply of crude oils. Conventional laboratory tests conducted to assess corrosivity of crude oils are complicated, expensive, and time-consuming; therefore, most of them are not convenient, taking into account the fast variability in the composition of the blends and the need to implement anticipated strategies for corrosion control.

For this reason, it is necessary to re-evaluate existing methods to quantify corrosion and propose new methodologies consistent with the dynamics of the refining industry. High-resolution nuclear magnetic resonance (NMR) spectra contain structural information on compounds and mixtures. In complex mixtures, such as crude oils, NMR makes it possible to determine the average structural parameters representing their intrinsic nature.<sup>9</sup> Statistical methods have been used in the past to correlate results from NMR with properties of crude oils and distillation cuts, such as boiling point, specific gravity, octane number, and the contents of saturates, aromatics, resins, and asphaltenes (the so-called SARA test), to generate chemometric prediction correlations.<sup>10,11</sup> Considering that the NMR spectra contain information on the structural nature of the crude oil and its corrosive species, the spectra collected from several crude oils could be correlated with corrosion rates determined by laboratory exposure tests to generate a correlation for predicting the corrosivity of crude oil. This prediction correlation could be more sensitive to variations in the composition of the mixtures entering the CDU and enables a

Received: June 24, 2015

Revised: October 27, 2015

Published: October 28, 2015

faster response to those variations. In this work, a wide variety of crude oils ranging from light to heavy was studied. The corrosivity of crude oils, determined to specific laboratory conditions, was correlated with its respective information from the  $^1\text{H}$  NMR spectrum, using chemometric methods. This correlation was statically evaluated and compared to a correlation that only takes into account the TAN and % SUL of crude oils.

## 2. EXPERIMENTAL SECTION

**2.1. Corrosion Tests.** Rectangular carbon steel AISI SAE 1005 coupons having dimensions of 7.62 cm length, 1.0 cm width, and 0.16 cm thickness were used for exposure tests according to the ASTM G-31 standard practice for laboratory immersion corrosion testing of metals.<sup>12</sup> The chemical composition of the carbon steel was analyzed by optical emission spectroscopy. For the corrosion tests, 44 samples of crude oils were used. The ranges of the physicochemical properties of the crude oil samples are shown in Table 1. The wide heterogeneity

**Table 1. Variation of the Physicochemical Properties of the Crude Oil Samples**

property	minimum	maximum
API gravity (deg)	12.4	44.6
total acid number (TAN)	0.00	6.84
weight percent of sulfur (% SUL)	0.06	2.24

of the physicochemical properties of the crude oil samples enables the correlation for predicting corrosivity to be applied to a broad range of crude oil mixture types.

The corrosion tests consisting in weight loss tests were conducted in an autoclave constructed of Hastelloy C276 at 350 °C. Before every test was started, the specimen was mechanically ground using emery paper 1500 grit, cleaned with deionized water, degreased with acetone, and dried in hot air. The dimensions of each coupon were then measured with a caliper, and the weight was determined using a precision balance. The specimens were exposed to the crude oil for 12 h. After each test, the coupons were cleaned ultrasonically with acetone, and subsequently, the corrosion products were removed according to the ASTM G-1 standard practice for preparing, cleaning, and evaluating corrosion test specimens using a mixture of 3.5 g of hexamethylenetetramine and 500 mL of 37 wt % hydrochloric acid, balanced with double-distilled water to make up a solution of 1000 mL.<sup>13</sup> The corrosion rate (CR) was determined on the basis of the total material loss, and it was expressed in millimeters per year using the following expression:

$$\text{CR} = \frac{K\Delta w}{ATD} \quad (4)$$

where  $K$  is a constant ( $8.76 \times 10^4$  to express corrosion in millimeters per year),  $\Delta w$  corresponds to the weight loss in grams,  $A$  corresponds to the area in centimeters squared,  $T$  corresponds to the test duration in hours, and  $D$  ( $\text{g}/\text{cm}^3$ ) corresponds to the density of the investigated carbon steel ( $7.8 \text{ g}/\text{cm}^3$ ). Three coupons were simultaneously tested in each exposure test, and the average value of the CR for these three coupons was used.

**2.2.  $^1\text{H}$  NMR Measurements.** The  $^1\text{H}$  NMR spectra of the crude oils were obtained using a Bruker Avance III 400 MHz spectrometer in 5 wt % solutions of  $\text{CDCl}_3$  containing tetramethylsilane (TMS) as the internal reference. Pulses of  $30^\circ$  with a pre-scan delay of  $10.0 \mu\text{s}$  was used, and the delay time between the scans was 10 s. The sweep width was 6000 Hz, and the acquisition time was 5.45 s. In total, 32 scans were averaged for each spectrum and used for the statistical analysis. The phase and baseline of the resulting spectra were manually adjusted and corrected. The phase of the spectrum needs to be corrected if the baseline around the peaks is not flat. In this point, the autophase routine does a pretty good job but it is likely that the spectrum will still need a little manual phasing to obtain a really good phase. Our

experience has shown that this automatic mode generally works well when pure compounds are analyzed; however, in the case of complex mixtures, such as crude oils, the phase obtained from the autophase mode is not good, and this must be performed manually. Manual phasing requires two phasing adjustments: the so-called zero- and first-order phase parameters. The zero-order phase adjustment affects the phasing of all of the peaks in the spectrum equally. The first-order correction varies linearly across the spectrum, so that the correction affects the peaks differently. The zero-order correction is used by adjusting the phase of one signal in the spectrum as judged “by eye”, and the first-order correction is then used by adjusting the phase of a signal far away from the first in a similar manner. Therefore, to achieve high accuracy, the phase, baseline, parts per million (ppm) scale, and integration were conducted 6 times for each spectrum; thus, the area of each chemical shift (H1, H2, ..., H12; see Table 2) is the averaged

**Table 2. Chemical Shift Regions in the  $^1\text{H}$  NMR Spectra of Crude Oils and Structural Assignments**

chemical shift (ppm)	nomenclature	hydrogen type
0.5–1.0	H1	$\text{CH}_3$ of paraffins ( $n$ - and iso); paraffinic hydrogen $\gamma$ and more to aromatic systems
1.0–1.7	H2	$\text{CH}_2$ of paraffins ( $n$ - and iso), CH of isoparaffins, CH and $\text{CH}_2$ of naphthenes; paraffinic hydrogen $\beta$ to aromatic systems
1.7–1.9	H3	CH and $\text{CH}_2$ of naphthenes; mostly $\beta$ -CH and $\beta$ - $\text{CH}_2$ to aromatic systems
1.9–2.1	H4	$\alpha$ - $\text{CH}_2$ to olefins
2.1–2.4	H5	$\alpha$ - $\text{CH}_3$ to aromatic carbons
2.4–3.5	H6	$\alpha$ -CH and $\alpha$ - $\text{CH}_2$ to aromatic carbons
3.5–4.5	H7	bridged $\text{CH}_2$ or CH
4.5–6.0	H8	CH and $\text{CH}_2$ of olefins
6.0–7.2	H9	CH of monoring aromatics
7.2–8.3	H10	CH of di-ring aromatics and some tri- and tetra-ring aromatics
8.3–8.9	H11	CH of some tri- and tetra-ring aromatics
8.9–9.3	H12	CH of some tetra-ring aromatics

result of six integrations. The integration was performed within each of these spectral segments, minimizing the small shifts observed from sample to sample. This was achieved by carefully setting the TMS signal to 0 ppm and normalizing the resulting integrals of the different segments of the spectrum. The spectrum was divided into 12 regions, as shown in Table 2 and Figure 1, based on recommendations from different authors.<sup>14–22</sup> Each of these spectral regions encompasses well-defined atomic groups, although some minor overlapping may

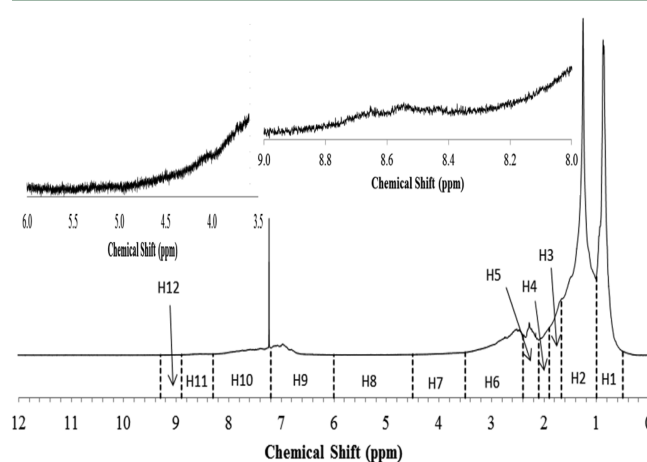


**Figure 1.**  $^1\text{H}$  NMR spectra of crude (TAN of 6.84) and the spectral partition according to the different chemical shifts.

still be present. The integration of these regions was then associated with the CR through partial least squares (PLS).

The chemical shift of acid protons (10–12 ppm) was not observed in  $^1\text{H}$  NMR spectra, even for high acid crude oil. This is due to the low abundance of protons associated with carboxylic groups. The NMR frequency of a nucleus in a molecule is determined principally by its gyromagnetic ratio and the strength of the magnetic field of the spectrometer; and resonance frequency also, slightly, depends upon the chemical environment of the nucleus in a molecule (the chemical shifts). In organic acids, the signal of protons adjacent to carboxylic groups is deshielded and changes the chemical shifts in the spectrum to downfield. It is a well-established fact that the chemical shifts observed in proton resonances reflect differences in the electron distribution about chemically non-equivalent proton and depend upon the neighbor substituent. In this case, the carboxylic group ( $-\text{COOH}$ ) changes the chemical shift of neighbor protons to downfield; for example, in alkanes, the  $\text{CH}_2$  changes approximately to 1.41 ppm.<sup>23</sup> In alkenes, vinyl protons ( $\text{C}=\text{C}-\text{H}$ ) change with respect to the position: 1.00 ppm for geminal, 1.35 ppm for *cis*, and 0.74 ppm for *trans* positions.<sup>24</sup> In aromatics, the relative position in substituted benzenes of the aromatic protons is affected as follows: *ortho*, 0.85 ppm; *meta*, 0.18 ppm; and *para*, 0.21 ppm.<sup>25</sup> Therefore,  $^1\text{H}$  NMR spectra contain information on the concentration of corrosive species and their respective structural nature.

**2.3. Statistical Analysis.** The correlation between the experimentally obtained CRs and the  $^1\text{H}$  NMR spectra of the crude oils was determined using the PLS regression method. From the 44 analyzed crude oil samples, 40 samples were randomly selected and used for the correlation. The additional 4 samples were used for external validation. The PLS regression method involves two steps, as described in ref 10: (1) training and (2) a prediction run. In the first step, the method requires the response spectrum  $x$  (i.e., the 12 frequency bins of the  $^1\text{H}$  NMR spectra) and a property  $q$  (CR) for each of the crude oil samples. The procedure for a particular property (CR) will be outlined here to show the different steps involved in the correlation between the areas of the NMR signals and properties. The notation employed is such that the area NMR1 (H1) of crude oil 1 is 1H1, while area 2 for the same crude oil is 1H2, etc. For crude oil 2 and H1 area, it will be 2H1, etc. These values formed the matrix  $x$ , while the different properties generated the matrix  $q$ , as shown in Scheme 1.

**Scheme 1. Matrix To Determine the Weight of Each Area of Integration**

$$x = \begin{bmatrix} 1\text{H1} & 1\text{H2} & 1\text{H3} & 1\text{H4} & 1\text{H5} & 1\text{H6} & 1\text{H7} & 1\text{H8} & 1\text{H9} & 1\text{H10} & 1\text{H11} & 1\text{H12} \\ 2\text{H1} & 2\text{H2} & \dots & & & & & & & & & 2\text{H12} \\ 3\text{H1} & & & & & & & & & & & \\ \vdots & & & & & & & & & & & \\ 40\text{H1} & \dots & & & & & & & & & & 40\text{H12} \end{bmatrix}; \quad q = \begin{bmatrix} 1.24 \\ 1.32 \\ 1.82 \\ \dots \\ \dots \\ 1.34 \end{bmatrix}$$

The application of PLS produces the weights ( $W_i$ ) for the different areas. In the present case, the results are shown in Table 3.

With Table 3 and matrix  $x$ , the factors ( $C_i$ ) were calculated as described in eqs 5 and 6.

$$C1 \text{ of crude oil 1} = (-0.0086 \times 1\text{H1}) + (-0.0082 \times 1\text{H2}) + (0.0111 \times 1\text{H3}) + \dots + (0.0019 \times 1\text{H12}) = 0.5294 \quad (5)$$

$$C10 \text{ of crude oil 40} = (0.0001 \times 40\text{H1}) + (-0.0035 \times 40\text{H2}) + (-0.0026 \times 40\text{H3}) + \dots + (0.0023 \times 40\text{H12}) = -0.1247 \quad (6)$$

During the training step, the PLS regression equations were repeatedly employed using an incremental number of factors. The more the factors are considered, the more the structure in  $x$  is used to build the relationship with the specific property  $q$ . The use of a few factors excludes valuable information and negatively affects the accuracy of the prediction correlation. As suggested by Molina et al.,<sup>10</sup> the best correlation was chosen on the basis of the prediction accuracy and the number of PLS factors employed. In this study, the use of 10 factors ( $C1$ – $C10$ ) for the CR provided the best prediction accuracy. The values for  $C_i$  for each crude are shown in Table 4.

$C1$ ,  $C2$ , ...,  $C10$  are taken as independent variables, and the CR is taken as a dependent variable, for a PLS regression. Several correlations with different  $C_i$  were considered. To select the optimal model in each case, the predicted residual sum of squares (PRESS) for the cross-validated models was computed with various numbers of factors. A leave-one-out cross-validation (CV) regression method was employed to estimate the prediction statistics. This is a strict validation tool, and it easily selects the best models. According to this procedure, the best prediction model is the one that has the largest  $\text{CV} - q^2$  value.<sup>23–28</sup> In addition, using the same number of samples (44), a linear correlation that relates the CR with the TAN and % SUL was determined to establish the advantages of the prediction correlation based on  $^1\text{H}$  NMR data. The accuracy of the correlations was established by evaluating the percentage root-mean-square error of prediction (% RMSEP), the percentage root-mean-square error of calibration (% RMSEC), the correlation coefficients ( $R^2$  and adjusted  $R^2$ ), and the correlation efficiency (EF).<sup>17</sup> The statistical parameters were determined from the following equations:

$$\text{RMSE} = \sqrt{\sum_{i=1}^n \frac{(y_i - y')^2}{n}} \quad (7)$$

$$\% \text{RMSE} = 100 \left( \frac{\text{RMSE}}{y'_i} \right) \quad (8)$$

$$\text{EF} = 1 - \frac{\sum_{i=1}^n (y' - y_i)^2}{\sum_{i=1}^n (y_i - y'_i)^2} \quad (9)$$

**Table 3. Weight of Variables  $x$**

	W1	W2	W3	W4	W5	W6	W7	W8	W9	W10
H1	−0.0086	−0.0055	−0.0149	−0.0057	−0.0001	0.0016	0.0001	0.0065	−0.0011	0.0001
H2	−0.0082	0.0017	0.0096	0.00477	−0.0034	−0.005	−0.0037	−0.0064	0.0003	−0.0035
H3	0.0111	0.0080	0.0006	−0.0022	−0.0074	−0.0141	−0.0133	−0.0022	−0.0031	−0.0026
H4	0.0112	0.0073	0.0031	0.0023	0.0039	0.0013	0.0025	0.0100	0.0085	−0.0011
H5			0.0003	−0.0026	−0.0013	0.0056	−0.0024	−0.0052	0.0002	−0.0009
H6				0.0067	0.0138	0.0148	0.0169	0.0059	0.0013	0.0068
H7						−0.0042	−0.0052	−0.0067	−0.0172	−0.0114
H8							0.0013	0.0123	0.0130	0.0124
H9								−0.0079	−0.0020	−0.0066
H10									−0.0026	0.0109
H11										−0.0112
H12	0.0019	−0.0052	0.0041	0.0165	0.0099	−0.0001	−0.0044	−0.0044	−0.0028	0.0023

Table 4.  $C_i$  Factors

crude oil	C1	C2	C3	C4	C5	C6	C7	C8	C9	C10	CR
1	-0.5294	-0.0069	0.0691	0.0580	-0.1540	-0.2099	-0.1424	-0.1555	-0.0183	-0.1570	1.2370
2	-0.4743	0.0382	0.0956	0.0708	-0.1477	-0.2018	-0.1246	-0.1592	-0.0162	-0.1510	1.3177
3	-0.3724	0.0513	0.0578	0.0526	-0.1039	-0.1526	-0.0618	-0.1239	-0.0174	-0.1166	1.8191
40	-0.4390	0.0230	0.0262	0.0474	-0.1355	-0.1780	-0.0966	-0.1254	-0.0219	-0.1247	1.3670

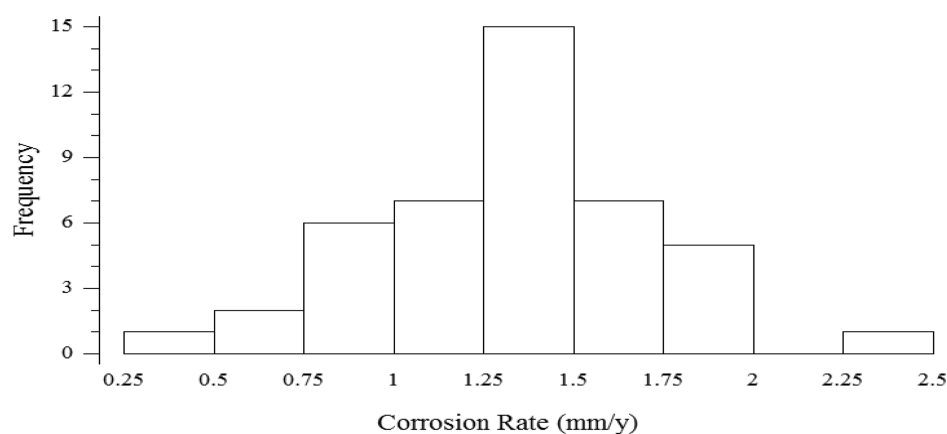


Figure 2. Distribution of the CRs (millimeters per year) for the samples used in this study.

where  $y'$  is the value predicted by the correlation,  $y_i$  is the measured value,  $n$  is the number of measurements,  $y_i'$  is the mean of the measured values. It is possible to estimate the accuracy of the simulations based on the % RMSE value.<sup>17,18</sup> A correlation is considered excellent when the % RMSE is less than 10%, good when  $10 \leq \% \text{RMSE} < 20$ , acceptable when  $20 < \% \text{RMSE} \leq 30$ , and not so exact when the % RMSE is more than 30%.<sup>25</sup> In the same way, a correlation is considered efficient when efficiency is greater than 0.6.

### 3. RESULTS AND DISCUSSION

The chemical composition of the carbon steel was found to be 0.055 wt % C, 0.172 wt % Mn, 0.0087 wt % P, 0.047 wt % Al, and 0.025 wt % Cr. The distributions of the CRs for 44 samples are shown in Figure 2.

From the chemometric analysis of the  $^1\text{H}$  NMR spectra, correlations were obtained by PLS; however, only the best are shown in this paper, i.e., the one with the best statistical parameters. The resulting equation for the prediction of the CR obtained from the PLS correlations of the  $^1\text{H}$  NMR data is shown in eq 10. More details about how to calculate these equations are reported in section 2.3 in this study. The correlation for predicting the CR using  $^1\text{H}$  NMR data and PLS methods is presented in eq 10

$$\begin{aligned} \text{CR} = & 0.35 - 1.06 \times \text{C3} - 5.77 \times \text{C4} - 15.82 \times \text{C5} \\ & + 5.82 \times \text{C7} + 1.10 \times \text{C4} \times \text{C4} - 29.32 \times \text{C9} \\ & \times \text{C9} + 2.99 \times \text{C10} \times \text{C10} + 0.15 \times \text{C2} \times \text{C3} \\ & - 5.06 \times \text{C5} \times \text{C6} + 2.08 \times \text{C6} \times \text{C7} \\ & - 0.47 \times \text{C7} \times \text{C8} + 5.99 \times \text{C9} \times \text{C10} \\ & - 0.27 \times \text{C1} \times \text{C4} + 1.00 \times \text{C1} \times \text{C5} \\ & + 0.95 \times \text{C1} \times \text{C6} - 2.39 \times \text{C1} \times \text{C10} \end{aligned} \quad (10)$$

Where CR is expressed in millimeters per year and C1, C2, C3, C4, ..., C10 are PLS factors. The relationship between TAN and % SUL with the CR is shown in Figures 3 and 4, respectively,

where there is a tendency to increase the CR with increasing TAN and % SUL in crude oils.

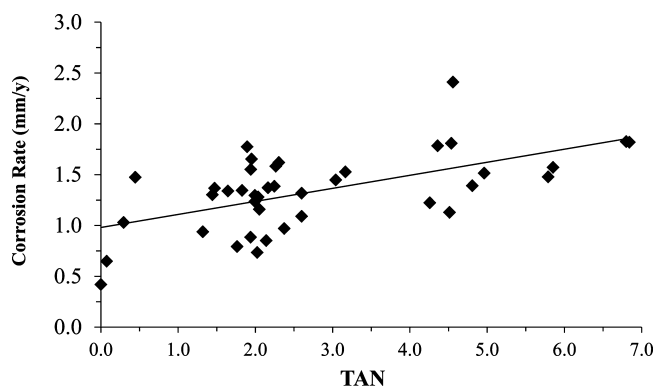


Figure 3. Effect of the acidity on the CR (millimeters per year).

The basic correlation for predicting corrosion obtained using information on the previous figures is presented in eq 11

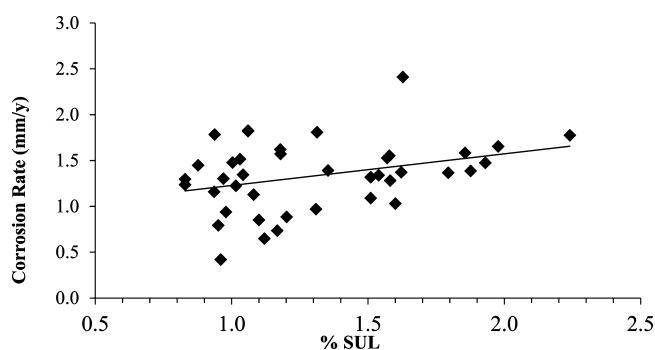


Figure 4. Effect of the sulfur compound content on the CR (millimeters per year).



$$CR = 0.23 + 0.15 \times TAN + 0.52 \times \% SUL \quad (11)$$

where CR (millimeters per year) is the corrosion rate, TAN is the total acid number, and % SUL (weight percent) is the sulfur content in the crude. TAN and % SUL are properties measured in the crude oil before carrying out the corrosion tests. In the above correlation, proportionality between the CR with TAN and % SUL is assumed, which is consistent with the rule of thumb used in the petroleum industry to predict the corrosivity of crude oils. However, this basic correlation cannot differentiate the corrosivity of crude oils with similar values of TAN and % SUL.

Table 5 shows the statistical parameters used to evaluate the quality of the correlations. All statistical parameters showed that

**Table 5. Statistical Evaluation of the Prediction Correlations of CR**

parameter	basic correlation	$^1\text{H}$ NMR correlation
$R^2$ (%)	55.72	92.53
adjusted $R^2$ (%)	55.43	87.33
CV - $q^2$	0.51	0.93
% RMSEC	46.04	16.24
% RMSEP	52.85	20.69
EF	0.27	0.92

the chemometric correlation based on the  $^1\text{H}$  NMR spectra has more accuracy than the correlation that only uses the concentration of TAN and % SUL

Figures 5 and 6 show the experimental and predicted CR values with the  $^1\text{H}$  NMR and basic correlations, respectively.

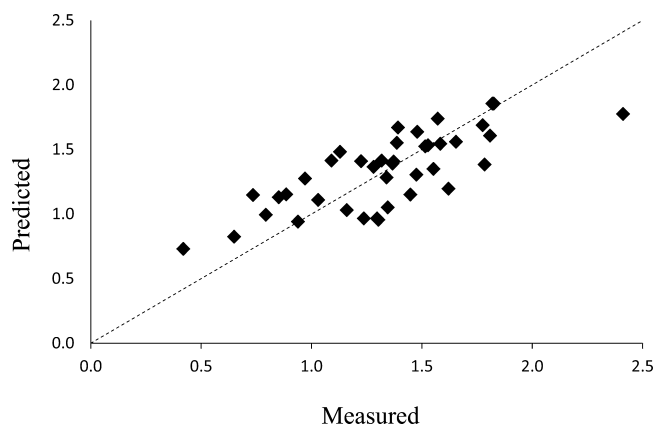


**Figure 5.** Experimental and predicted CRs (millimeters per year) using the basic correlation.

Despite being a pure statistical correlation, the  $^1\text{H}$  NMR model involves the structural heterogeneity of the crude oils and corrosive species. This is an advantage that allows for the model to detect differences in the corrosivity of crude oils, even when they have similar concentrations of TAN and % SUL.

#### 4. CONCLUSION

The use of  $^1\text{H}$  NMR spectra and chemiometric methods provides a notably fast method to predict the corrosion tendency for a wide variety of crude oils. All statistical parameters showed that the  $^1\text{H}$  NMR-based correlation has a more accurate prediction than the model correlating the CR with the TAN and % SUL. Although it is a statistical correlation, the  $^1\text{H}$  NMR correlation takes into account the

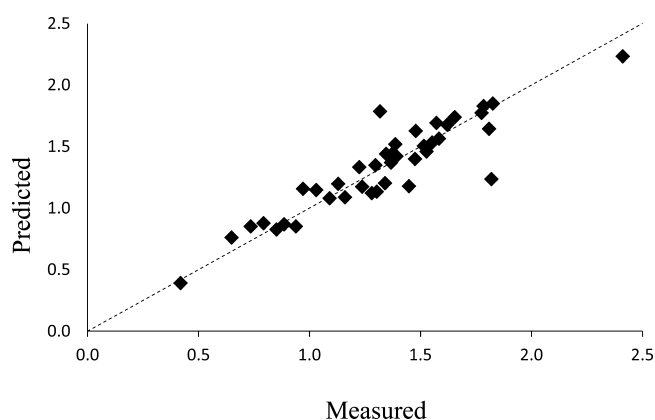


**Figure 6.** Experimental and predicted CRs (millimeters per year) using  $^1\text{H}$  NMR correlation.

structural heterogeneity of the corrosive species. Therefore, the  $^1\text{H}$  NMR correlation could identify differences in the CRs for crude oil with the same TAN and % SUL. Refining engineers may obtain their own correlations to establish strategies for anticipated corrosion control from measurements of CRs calculated in the laboratory or directly at the refinery.

#### AUTHOR INFORMATION

##### Corresponding Author

\*E-mail: [caumejia@gmail.com](mailto:caumejia@gmail.com).

##### Notes

The authors declare no competing financial interest.

#### ACKNOWLEDGMENTS

The financial support from the Instituto Colombiano para el Desarrollo de la Ciencia (COLCIENCIAS) for the development of this project is acknowledged.

#### REFERENCES

- (1) Hart, A.; Leeke, G.; Greaves, M.; Wood, J. Down-hole heavy crude oil upgrading by CAPRI: Effect of hydrogen and methane gases upon upgrading and coke formation. *Fuel* **2014**, *119*, 226–235.
- (2) Qu, D. R.; Zheng, Y. G.; Jing, H. M.; Yao, Z. M.; Ke, W. High temperature naphthenic acid corrosion and sulphidic corrosion of Q235 and 5Cr1/2Mo steels in synthetic refining media. *Corros. Sci.* **2006**, *48*, 1960–1985.
- (3) Huang, B. S.; Yin, W. F.; Sang, D. H.; Jiang, Z. Y. Synergy effect of naphthenic acid and sulfur corrosion in crude oil distillation unit. *Appl. Surf. Sci.* **2012**, *259*, 664–670.
- (4) Dettman, H. D.; Li, N.; Luo, J. Refinery corrosion, organic acid structure, and Athabasca bitumen. *Corrosion* **2009**, Paper 09336.
- (5) Messer, B.; Tarleton, B.; Beaton, M.; Phillips, T. New theory for naphthenic acid corrosivity of Athabasca oil sands crudes. *Corrosion* **2004**, Paper 04634.
- (6) Tebbal, S.; Schutt, H.; Podlecki, R.; Sudhakar, C. Analysis and corrosivity testing of eight crude oils. *Corrosion* **2004**, Paper 04636.
- (7) Yépez, O. On the chemical reaction between carboxylic acids and iron, including the special case of naphthenic acid. *Fuel* **2007**, *86*, 1162–1168.
- (8) Freitas, S.; Malacarne, M. M.; Romão, W.; Dalmascio, G. P.; Castro, E. V. R.; Celante, V. G.; Freitas, M. B. J. G. Analysis of the heavy oil distillation cuts corrosion by electrospray ionization FT-ICR mass spectrometry, electrochemical impedance spectroscopy, and scanning electron microscopy. *Fuel* **2013**, *104*, 656–663.
- (9) Poveda, J. C.; Molina, D. R. Average molecular parameters of heavy crude oils and their fractions using NMR spectroscopy. *J. Pet. Sci. Eng.* **2012**, *84–85*, 1–7.

- (10) Molina V, D.; Uribe, U. N.; Murgich, J. Correlations between SARA fractions and physicochemical properties with  $^1\text{H}$  NMR spectra of vacuum residues from Colombian crude oils. *Fuel* **2010**, *89*, 185–192.
- (11) Muhammad, A.; Azeredo, R. B. V.  $^1\text{H}$  NMR spectroscopy and low-field relaxometry for predicting viscosity and API gravity of Brazilian crude oils – A comparative study. *Fuel* **2014**, *130*, 126–134.
- (12) ASTM International. *ASTM G1-03. Standard Practice for Preparing, Cleaning, and Evaluating Corrosion Test Specimens*; ASTM International, West Conshohocken, PA, 2011.
- (13) ASTM International. *ASTM G31-12a. Standard Guide for Laboratory Immersion Corrosion Testing of Metals*; ASTM International, West Conshohocken, PA, 2012.
- (14) Gillet, S.; Delpuech, J. J.; Valentin, P.; Escalier, J. C. Optimum conditions for crude oil and petroleum product analysis by carbon-13 nuclear magnetic resonance spectrometry. *Anal. Chem.* **1980**, *52*, 813–817.
- (15) Gillet, S.; Rubini, P.; Delpuech, J. J.; Escalier, J. C.; Valentin, P. Valentin, Quantitative carbon-13 and proton nuclear magnetic resonance spectroscopy of crude oil and petroleum products. 2. Average structure parameters of representative samples. *Fuel* **1981**, *60*, 221–225.
- (16) Brown, J. K.; Ladner, W. R. Hydrogen distribution in coal-like materials by high-resolution nuclear magnetic resonance spectroscopy. *Fuel* **1960**, *39*, 87–96.
- (17) Rongbao, L.; Zengmin, S.; Bailing, L. Structural analysis of polycyclic aromatic hydrocarbons derived from petroleum and coal by  $^{13}\text{C}$  and  $^1\text{H}$  NMR spectroscopy. *Fuel* **1988**, *67*, 565–569.
- (18) Kapur, G. S.; Singh, A. P.; Sarpal, A. S. Analysis of hydrocarbon mixtures by diffusion-ordered NMR spectroscopy. *Fuel* **2000**, *79*, 1023–1029.
- (19) Sarpal, A. S.; Kapur, G. S.; Mukherjee, S.; Tiwari, A. K. PONA analyses of cracked gasoline by  $^1\text{H}$  NMR spectroscopy. Part II. *Fuel* **2001**, *80*, 521–528.
- (20) Ha, Z.; Ring, Z.; Liu, S. Quantitative Structure-Property Relationship (QSPR) Models for Boiling Points, Specific Gravities, and Refraction Indices of Hydrocarbons. *Energy Fuels* **2005**, *19*, 152–163.
- (21) Kapur, G. S.; Ecker, A.; Meusinger, R. Establishing Quantitative Structure-Property Relationships (QSPR) of Diesel Samples by Proton-NMR & Multiple Linear Regression (MLR) Analysis. *Energy Fuels* **2001**, *15*, 943–948.
- (22) Meusinger, R. Gasoline analysis by  $^1\text{H}$  nuclear magnetic resonance spectroscopy. *Fuel* **1996**, *75*, 1235–1243.
- (23) Shoolery, J. N. *Varian Technical Information Bulletin*; Varian Associates: Palo Alto, CA, 1959.
- (24) Crews, P.; Rodriguez, J.; Jaspars, M. *Organic Structure Analysis*; Oxford University Press: New York, 1998.
- (25) Corio, P. L.; Dailey, B. P. Relative electron densities in substituted benzenes. *J. Am. Chem. Soc.* **1956**, *78* (13), 3043–3048.
- (26) Montgomery, D. C.; Runger, G. C. *Applied Statistics and Probability for Engineers*; John Wiley and Sons: New York, 2003.
- (27) Otto, M. *Chemometrics. Statistics and Computers, Application in Analytical Chemistry*; Wiley-VCH: New York, 1999.
- (28) Jago, G.; Bélanger, G.; Tremblay, G. F.; Jing, Q.; Baron, V. S. Calibration and performance evaluation of the STICS crop model for simulating. *Field Crops Res.* **2013**, *151*, 65–77.